Laboratory study on thermal performance of natural air convection in porous media

Jianfeng Chen
Golder Associates Ltd., Burnaby, BC, Canada
Lukas Arenson
BGC Engineering Inc., Vancouver, BC, Canada
David C. Sego
Department of Civil and Environmental Engineering – University of Alberta, Edmonton, AB, Canada

ABSTRACT
This study focussed on a detailed understanding of the characteristics of natural air convection in porous media. Heat transfer experiments were carried out using a well-insulated cylindrical tank filled with Styrofoam chips. Convection and conduction were caused by controlling the boundary temperatures at the top and bottom of the tank, and a number of cross-sectional conductive and convective isotherms were generated from collected temperature data. Convective patterns were also obtained from tests by centrally localized heating from the bottom or cooling from the top of the tank. Air flow velocities were measured at the center of the tank.

RÉSUMÉ
Cette étude s'est concentrée sur un arrangement détaillé des caractéristiques de la convection naturelle d'air dans des milieux poreux. Les expériences de transfert thermique ont été effectuées en utilisant un réservoir cylindrique rempli de morceaux de mousse de polystyrène. La convection et la conduction ont été provoquées par les températures au dessus et au bas du réservoir. Un nombre d'isothermes conductrices et convectrices ont été produites des données rassemblées de la température. Des modèles convecteurs ont été obtenus à partir des essais par le chauffage centralement localisé du fond ou le refroidissement à partir du dessus du réservoir. Pareillement des vitesses de circulation d'air ont été mesurées au centre du réservoir.

1 INTRODUCTION

Convective air cooling in Arctic climates has been observed for decades and had been applied in cold regions geotechnical engineering design and practice for waste rock piles and road embankments. Natural air convection in porous media, extensively studied in mechanical and thermodynamical engineering (Nield and Bejan, 1999), is gradually becoming an important consideration in geotechnical engineering mainly because of the potential for high heat transfer rates. Protection of permafrost from thaw in cold regions is a critical design consideration for various civil facilities. Convective air movement in highly permeable material is more efficient at cooling the ground in winter, whereas in summer, thermal conduction with lower heat transfer rates dominates and therefore protects the ground from thawing. As such, an air convection embankment (ACE) constructed from poorly graded coarse material was called “thermal diode” by Goering and Kumar (1996), or “thermal semi-conductor” by Cheng et al. (2007). Harris and Pedersen (1998) performed a temperature monitoring study at the Plateau Mountain in Alberta and found that the mean annual ground temperatures in the blocky materials of that area were 4 to 7°C cooler than nearby mineral soils because of the air convective cooling effect. Practical application of ACE were reported by Cheng et al. (2008) and Xu and Goering (2008).

A number of experimental and numerical studies on the cooling effect of air convection in highly permeable embankments have been reported by Goering (1998; 2002; 2003), Goering et al. (2000), Yu et al. (2004), Sun et al. (2005), Ma et al. (2008), Jørgensen et al. (2008), and Wu et al. (2008). Arenson and Sego (2007) presented a numerical simulation showing that convection of cold winter air in a coarse mine waste rock cover for a tailings pond can be used to accelerate the freezing and potential stabilization of the tailings. In addition, Pham et al. (2008) conducted field temperature monitoring study and numerical modelling on mine waste rock piles located in the Northwest Territories, and showed that temperatures of the pile cores lowered by up to 5 °C in nine years due to cooling effects of natural convection.

Both conductive and convective heat transfer mechanisms must be fully understood when working on cold regions or permafrost engineering if poorly-graded materials are being used for construction (e.g., railway ballast embankments, rock fill dams, waste rock piles and tailings covers after mine closure). In the present study, a laboratory investigation of convective air heat transfer in a porous medium was carried out by using a cylindrical test tank. A variety of isotherms were obtained by measuring cross-sectional temperatures. Initial results of this laboratory study were published by Arenson et al. (2007). This paper presents succeeding test results based on adjusted experimental configurations.

2 TEST APPARATUS AND PROCEDURES

An insulated, cylindrical plastic tank filled with Styrofoam chips as a surrogate for porous media, was selected. The

cylindrical tank provided a radius to height ratio of 0.39 (Figure 1).

Controlled heating or cooling systems were installed at the top and bottom of the tank to create different top-to-bottom temperature boundary conditions, including localized heating at the bottom or cooling at the top, capable of inducing conductive and/or convective heat transfer. The selected Styrofoam was an S-shaped expanded polystyrene (EPS) fill with a measured solid density of 6.5 kg/m^3. It was naturally placed at a porosity of approximately 50%. The thermal conductivity of the Styrofoam was approximately 0.035 W/(m ·°C).

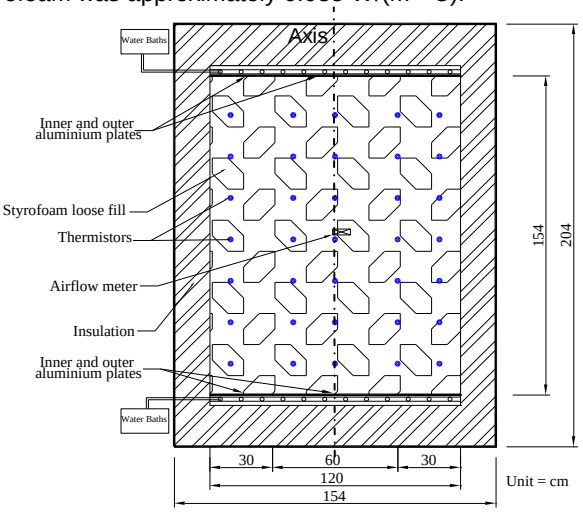

Figure 1. Schematic section of experimental system.

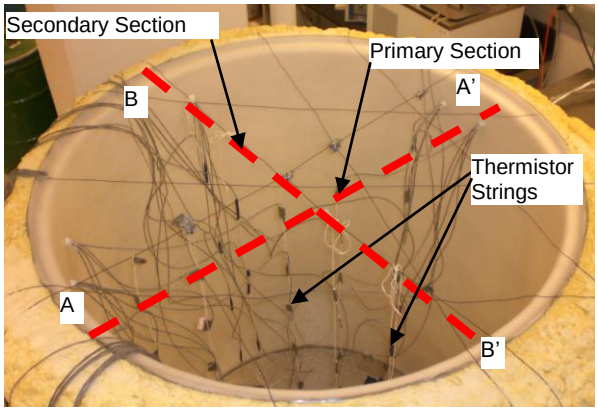

Figure 2. Photograph of test tank and instruments.

Figure 2 shows a photograph of the test tank and thermistor strings. A total of 56 thermistors were installed on the selected cross sections and the aluminum plates. Only the top and bottom temperature boundary conditions are changeable. The two cooling/heating systems at the top and bottom consisted of coils of copper tubing and were connected to constant temperature baths using plastic tubing. Heat transfer was capable between the copper tubing and the tank through two sets of attached aluminum plates at the top and bottom. Internal temperatures were measured at a number of locations on two perpendicular instrumentation sections (primary and secondary) within the tank. At the same time, vertical air flow velocities were measured by an air flow meter at the center of the tank. The air flow meter (0-0.51 m/s with 1.5% accuracy) contains two RTD (Resistance Temperature Detectors) elements with a constant temperature difference and obtains velocity readings based on a cooling effect of air flow to one RTD. The tip of the flow meter was protected from clogging of Styrofoam chips (Figure 3).

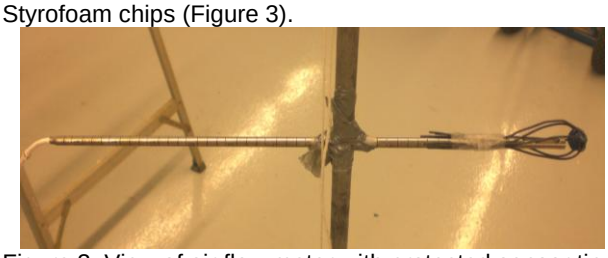

Figure 3. View of air flow meter with protected sensor tip.

In this study, heating from below represents increasing the bottom temperature to a certain value while the top temperature is maintained constant. Likewise, cooling from top refers to decreasing the top temperature to a certain value while the bottom temperature is kept constant. During localized heating on the bottom or cooling on the top of the tank, only the temperature of the inner circular plate (0.6 m in diameter) is changed while that of the outer plate is maintained constant.

3 RESULTS

Temperature and air flow velocity data were obtained from experiments of convection and conduction carried out in test tank filled with Styrofoam chips. Localized heating or cooling is applied in these convection tests. Contour plots were created based on linear interpolation between temperatures measured at various points within the tank.

Temperatures were normalized with respect to the minimum and maximum plate temperatures measured in the tank at steady state. The non-dimensional temperatures were generally in the range of 0 to 1. This facilitated comparisons of convection and conduction heat transfer tests with different top-to-bottom temperature boundary conditions.

Temperatures measured along section sides were used as boundaries on the contour plots, neglecting the distances between these thermistor strings and the tank wall. Temperatures measured on the top and bottom plates were averaged for contour construction except for localized heating and cooling tests where inner and outer plate temperatures were different.

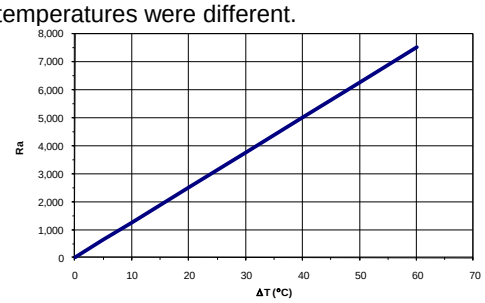

Figure 4. Onset Rayleigh number (Ra) versus top-to-bottom temperature difference (ΔT).

3.1 Convection

Natural convection starts when a Rayleigh number is larger than the critical Rayleigh number (Nield and Bejan, 1999), it is therefore necessary to estimate the Rayleigh numbers before performing the convection tests with a porous material to ensure air movement due to natural convection will occur.

As other parameters were kept constant during the tests, an onset Rayleigh number was a function of the top-to-bottom temperature difference assigned for the convection tests, and was calculated based on estimated intrinsic permeability and thermal conductivity of Styrofoam chips (Figure 4). The magnitudes of Rayleigh numbers were greater than the critical Rayleigh number of 39.5 that is suggested by Nield and Bejan (1999), and therefore implied that convective air movement would occur in the test tank under small top-to-bottom temperature differences (less than 0.5°C).

Steady state contours are shown in Figures 5 and 6 for tests using temperature differences of ΔT = 10°C, 20°C, and 30°C by either heating from below or cooling from top. Transient contour patterns for ΔT = 5 and 10°C have been reported by Arenson et al. (2007).

Heating from below normally led to a dual-cell pattern being formed during convection in the tank, i.e. air rising along an axis and sinking along the outer tank wall. For convection with higher Rayleigh numbers, the contours are steeper and the axis deflects from the centerline of the tank. The rising air flow plumes near the center of the tank also have higher values of non-dimensional temperatures (Figure 5).

Under the experimental conditions presented, it was observed that all tests with cooling from top lead to steady state unicellular convective flow patterns. It may be due to the conditions at the top seal that were different from the bottom. Air is sensitive to small temperature perturbation, thus the convective pattern varied with minor temperature changes. Comparing the contours on the left of the sections, the non-dimensional temperatures of the sinking air flow plumes are lower for the tests with higher Rayleigh numbers (Figure 6). Note that the contours at the lower right corner become denser from ΔT = 10°C to 30°C, illustrating that the cool air moved more effectively to the right wall and then rose. This demonstrates that convection with high Rayleigh numbers has higher convective heat transfer rates.

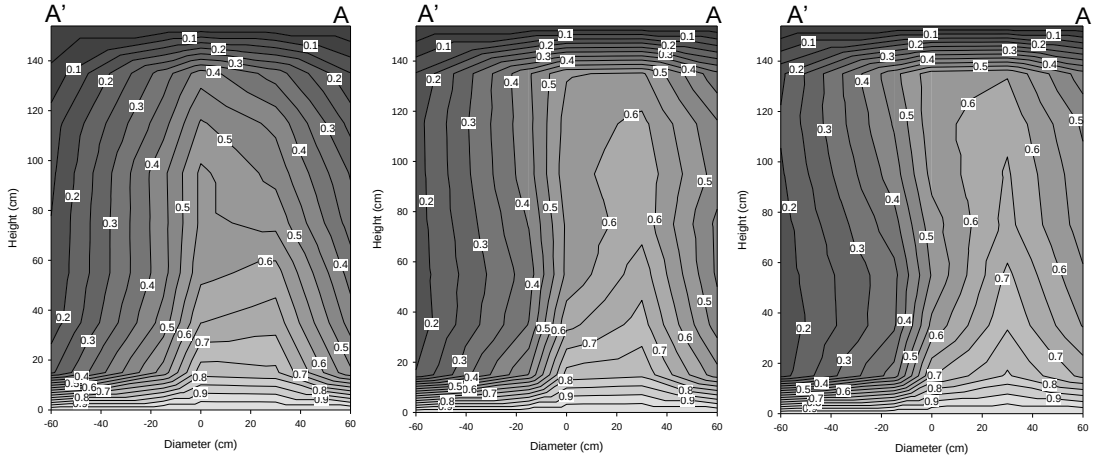

(a) ΔT = 10°C (B33-T23)* (b) ΔT = 20°C (B43-T23) (c) ΔT = 30°C (B53-T23)

Figure 5. Steady state convection non-dimensional isotherms for primary section (heating from below).

* Note: In figure titles of this paper, B# and T# denote bottom and top temperatures in °C; LB# and LT# denote temperatures for localized heating and cooling.

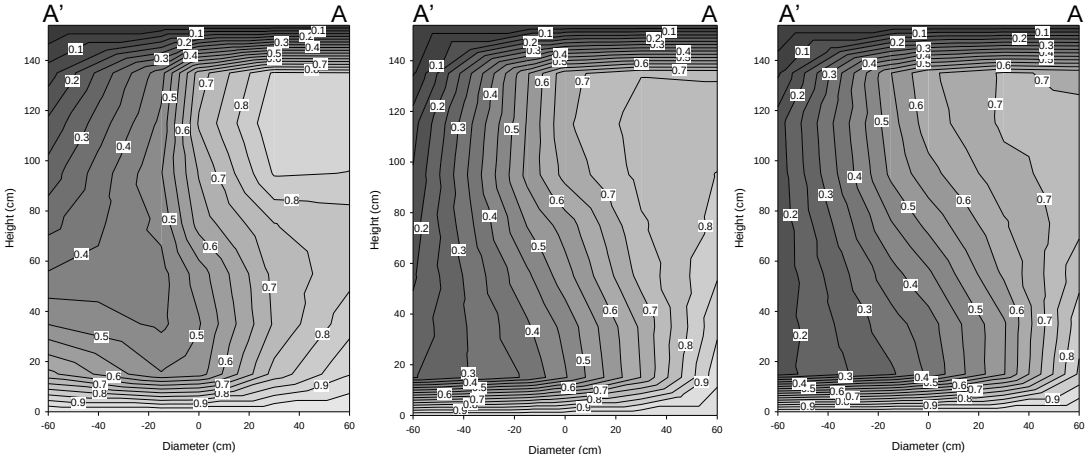

(a) ΔT = 10°C (B33-T23) (b) ΔT = 20°C (B43-T23) (c) ΔT = 30°C (B53-T23)

Figure 6. Steady state convection non-dimensional isotherms for primary section (cooling from top).

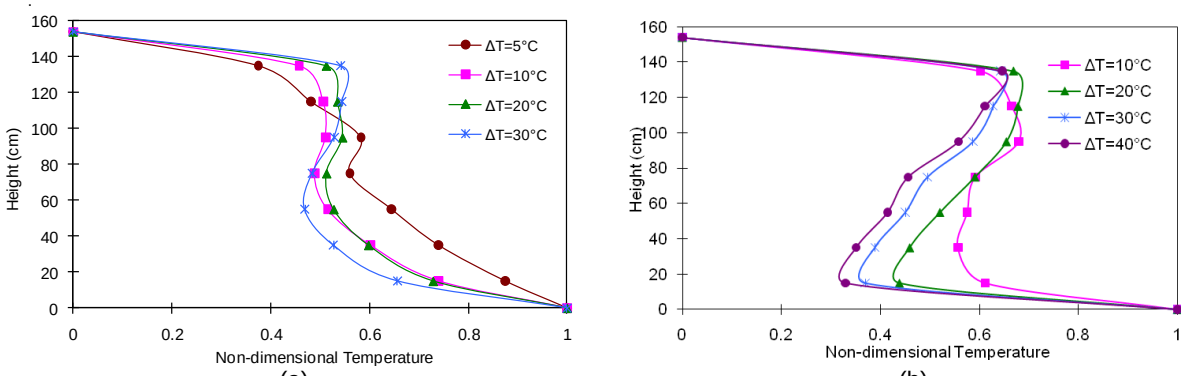

Figure 7. Steady state axial temperature profiles for convection by heating from below (a) and cooling from top (b).

Normalized axial temperature profiles at steady state for scenarios of heating from below and cooling from top are also different as shown in Figure 7. The patterns for convection by heating from below illustrate that the temperatures increased as the bottom temperature rose. Axial temperatures increase downwards with the height of the tank (Figure 7a). However, the curves for cooling from top case have non-monotonic characteristics such that the upper part axial temperatures were higher than the lower part (Figure 7b). This corresponds to the steady state contour patterns and was due to the unicellular convective pattern in which colder air is sinking along the right side of the tank.

The contour plots using data from the other sections can be used to confirm the air flow patterns. Figures 8a and 8b for the primary and secondary sections confirm the unicellular convection in the tank.

To investigate the convective cell orientation for a unicellular convective pattern, the top tubing coil (attached to top plates) was rotated approximately 45 degrees. The isotherms for the secondary section after rotation (Figure 8c) show that the convective air flow cell direction moved to a new position, which was likely following the position of the tubing inlet/outlet. This, in turn, shows that the temperature at the top initiated by the water entering the tubing may affect the direction of the unicellular convective cell within the tank. In other words, a convective air flow mode tends to form based on small disturbances of system inputs under the existing experimental conditions.

When a convection test of ΔT = 50°C (onset Ra = 6200) was carried out, temperature fluctuations and oscillations occurred. As shown in Figure 9a, temperatures along the axis fluctuated extensively. Oscillations were contained during the fluctuations and some points near the bottom underwent large variations. The plots illustrate that those oscillations with varying amplitudes were time dependent, and nearly disappeared by the end of the test.

Part of the temperature variation curves (approximately 80 minutes) is shown in Figure 9b, illustrating typical periods and amplitudes of the oscillations. The amplitude of each thermistor varies, and the largest was about 6°C for the thermistor T4, which was located near the center of the bottom. The period for T4 was approximately 25 minutes. The curve of T4 shows that the time taken during the variation from point 1 to 3 was longer than that from point 3 to 4, indicating that temperatures increased from trough to peak more quickly than those decreased from peak to trough in an oscillation period. This was more significant in higher amplitude curves of thermistors near the bottom such as T4, T1 and T2.

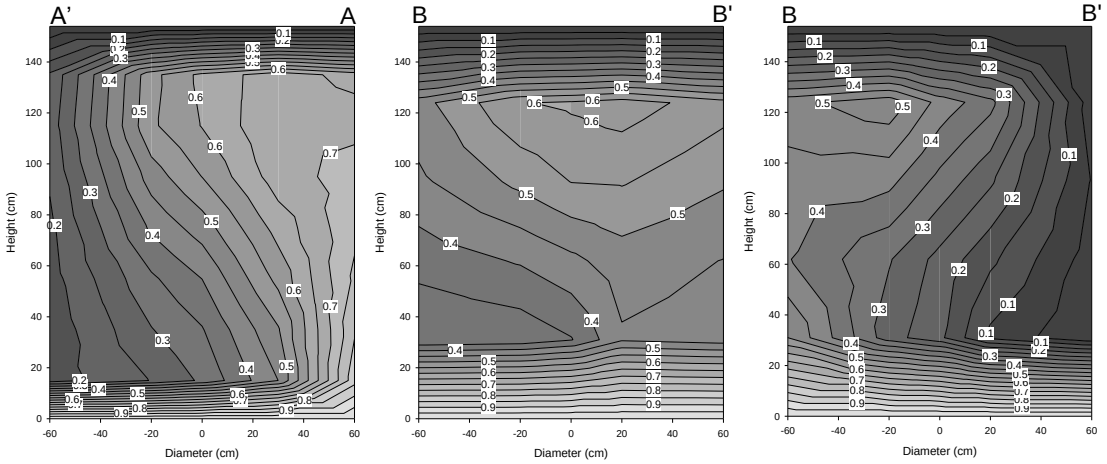

Figure 8. Steady state convective pattern variation at secondary section (ΔT = 40°C).

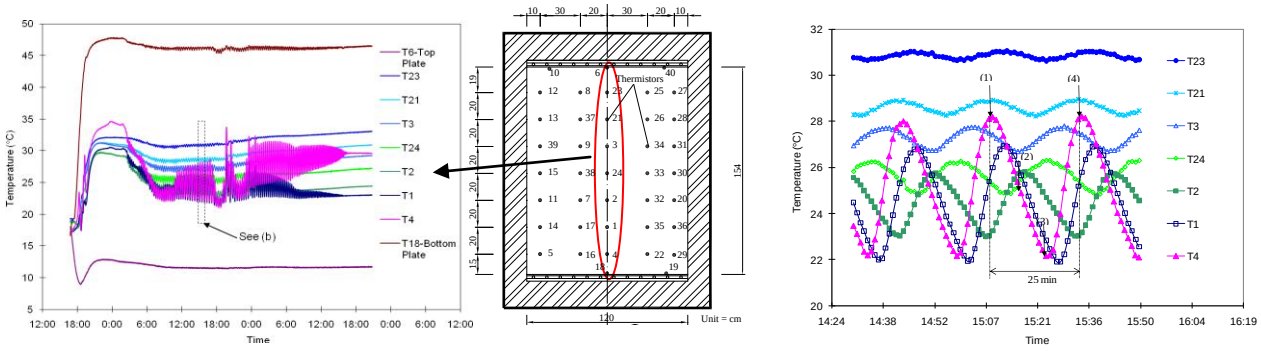

(a) (b)

Figure 9. Fluctuations and oscillations observed from convection test under ΔT = 50°C (B53-T3).

According to Horne and O'Sullivan (1978), this type of oscillation is due to high air flow acceleration caused by rapid temperature changes. Kladias and Prasad (1990) also concluded that higher Rayleigh numbers results in shorter oscillation periods.

However, only minor oscillatory instability was observed during the convection test of ΔT = 60°C (onset Ra = 7400), particularly for those points near the right side of the bottom plate. This confirms that oscillations have a time-dependent characteristic for this convection test system, and are difficult to predict.

3.2 Localized Heating or Cooling

Transient convective patterns from the primary instrumentation section for localized heating under ΔT = 10°C and localized cooling under ΔT = 10°C are presented in Figures 10 and 11.

The convective patterns were established in the first several hours and the overall temperatures in the tank continued to vary until steady state was reached. Heat plumes rose in the center of the tank with steep and more concentrated contours. Convection under higher ΔT had more compressed central isotherms, indicating higher air flow rates leading to higher heat transfer rate along the tank axis.

Steady state isotherms of the primary section for localized heating induced convection tests under ΔT = 10°C, 20°C and 30°C are presented in Figure 12. Localized heating apparently stabilizes the symmetry of the convective air flow in the tank as warm air is well confined to the center of the tank. Corresponding contours of the secondary section confirmed the better symmetry.

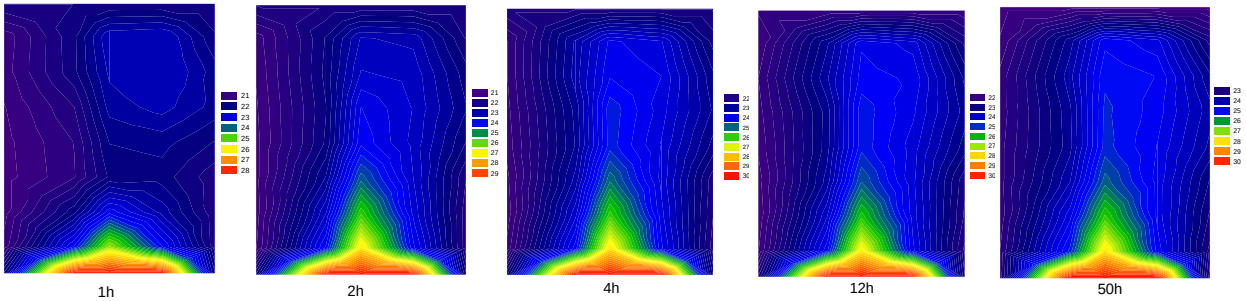

Figure 10. Transient convective isothermal patterns, ΔT = 10°C (LB32-22T), localized heating from below.

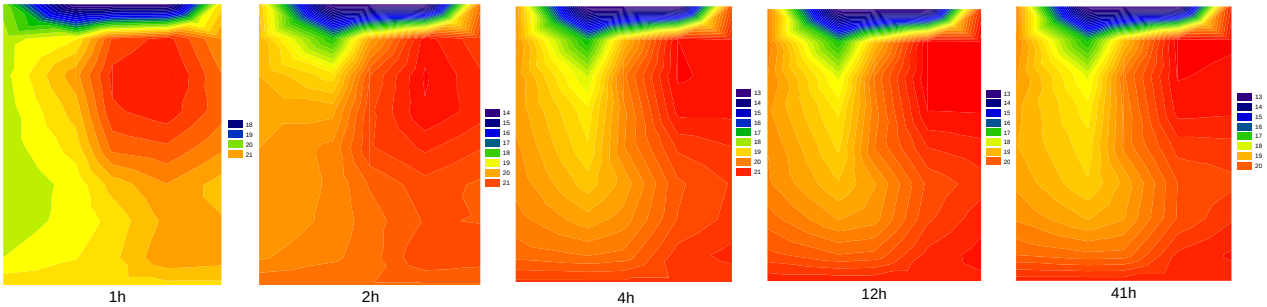

Figure 11. Transient convective isothermal patterns, ΔT = 10°C (B20.5-LT10.5), localized cooling from top.

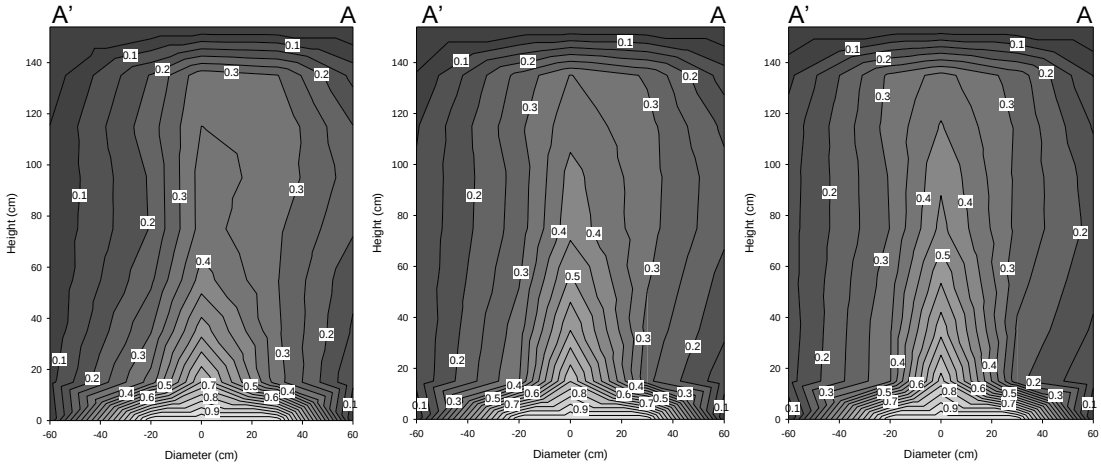

(a) ΔT = 10°C (LB32-T22) (b) ΔT = 20°C (LB42-T22) (c) ΔT = 30°C (LB52-T22)

Figure 12. Steady state convection non-dimensional isotherms for primary section (localized heating from below).

Dual-cell convection with poor symmetry was observed for Localized cooling from top under ΔT = 20°C (Figure 13), which is different from the unicellular convection obtained by cooling the full plate above.

Compared to the convection tests under a fully heated boundary at the bottom, the non-dimensional temperatures in the tank for localized heating tests are generally lower. This is because the heating or cooling source at the boundary was smaller and the energy input into the tank is also lower. As a result, heat transfer rates decreased for convection with localized heating under the same test conditions. Similarly, higher non-dimensional temperatures were observed in the tank for localized cooling tests compared to tests with a fully cooling boundary at the top.

In addition, temperature variations in the tank are stable for convection test with localized heating under ΔT = 60°C. No fluctuations and oscillations were observed. This further demonstrates that localized heating can stabilize the convective air movement, regardless of relatively high onset Rayleigh numbers.

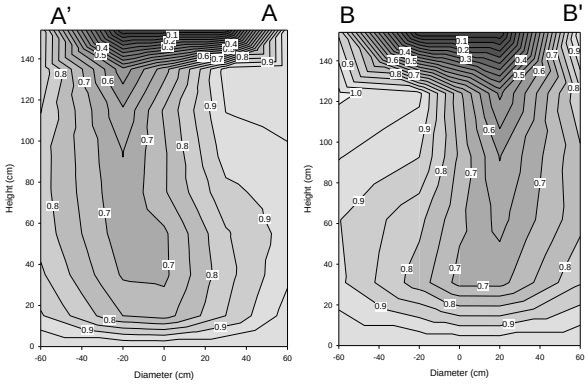

(a) Primary Section (b) Secondary Section

Figure 13. Steady state convection non-dimensional isotherms for primary section (localized cooling from top), ΔT = 20°C (B21-LT1.0).

3.3 Convective Air Flow Velocity

Air flow velocities measured at the center of the tank are directly related to the convective patterns. Since axial air flow for unicellular convection is not stable as observed from temperature contours during the tests by cooling from top, measuring vertically at the center of the tank is more suitable for axial symmetric flow with stable patterns than it is for unicellular convective flow.

It was noted that convection tests with localized heating from below have more stable air flow (temperature) pattern. Velocities recorded from those tests were used to illustrate that higher Rayleigh numbers result in higher flow velocity. For these tests with heating from below, flow velocity normally peaks then decreases to a relatively stable value. These velocity data from tests of localized heating are summarized in Figure 14, showing that peak and stable values increase with increasing ΔT under localized heating conditions. In this study, a maximum velocity of 0.068 m/s was observed for convective air flow in the pores formed by Styrofoam chips.

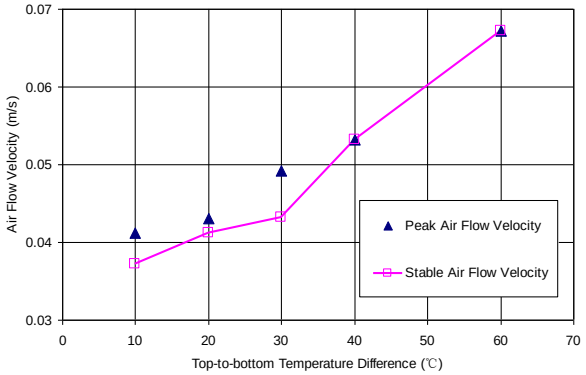

Figure 14. Measured air flow velocity versus temperature difference for convection by localized heating from below.

3.4 Thermal Conduction

After uniform temperatures were reached inside the tank, thermal conduction tests for the Styrofoam chip filled tank were started by increasing the top temperature. Temperatures gradually increased downward throughout the tank. Clear horizontal temperature stratifications were formed as illustrated by Arenson et al. (2007).

Figure 15 shows a vertical temperature profile varying with time for ΔT = 20°C. The profile slowly approaches the theoretical steady state that is a linear distribution through the Styrofoam chips. However, after even 42 hours of testing, the theoretical linear gradient in the tank was not reached. This is likely attributable to thermal insulation effects from Styrofoam and insufficient heat supply from the constant temperature baths in the test environment. Additional tests showed that, if the bottom is cooled at the same time, the steady state contours were closer to the theoretical condition. Heat transfer through the wall may also have impact on the internal system during these tests. As compared with convection tests, the ability to approach steady state is lower through thermal conduction. This illustrates that high heat transfer rates can be easily obtained from convection in a low thermal conductivity medium through convective air movement.

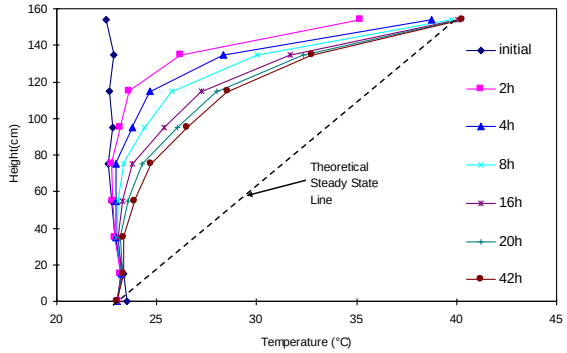

Figure 15. Axial temperature profile for thermal conduction test under ΔT=20°C (B23-T43).

3.5 Discussion

The Styrofoam chips with a low thermal conductivity (close to air) increased the Rayleigh number and therefore maximized the ability of convective air movement. However, the conductive heat exchange through the tank wall needs to be taken into consideration especially when attempting to model these measurements.

Rayleigh numbers estimated for this test system were high due to the use of the Styrofoam chips. As a result, a critical height of the tank required to induce natural convection under a temperature difference would be low if variable top-to-bottom heights were used. For example, the critical height would be about 0.1 m under ΔT=5°C to achieve the critical Rayleigh number for convection.

Once convection starts, critical gradients in a system should be another consideration. If the temperature gradient is small, then air convection would be ineffective due to slow convective air flow. Limitations of the insulation such as the conditions of the upper seal can cause unexpected temperature perturbation leading to unstable convective air movement that may affect the test results. For given test conditions, the limitations may impact convective pattern symmetry, convective cell number established, fluctuations and oscillations as well as time to reach steady state heat flow conditions.

Three-dimensional effects from the top and bottom plates and the shape of the tank may also affect the convective patterns such that the flow directions change when air flow contacts any uneven surface on the constant temperature plate and tank wall.

The capacity of the constant temperature baths was limited for heating or cooling the plates during these tests, particularly for those with larger top-to-bottom temperature differences. Circulating water through the tubing was associated with heat loss or gain, further influencing temperatures. Consequently, a temperature set on the bath was not necessarily identical to that recorded at the plate.

The limitations of this study included that only one medium material was tested; only one type of test enclosure (geometry) was used; and only one type of boundary condition was adopted. In fact, the complexity of air convection is significant, which is one of the reasons that air convection is often excluded from thermal studies for projects in current cold region engineering practice.

4 CONCLUSIONS

This laboratory study was intended to obtain a detailed understanding of the characteristics of natural air convection in a porous medium within a cylindrical tank, and to provide a concept that air convection in highly permeable material is applicable for cold region geotechnical engineering.

Based on the results from this laboratory investigation, the following can be concluded:

1. Convective heat transfer through air movement is more efficient than thermal conduction for this particular experimental system using low-thermal conductivity media.
2. Convection with a higher Rayleigh number has a higher heat transfer rate.
3. Convective patterns for natural air convection in a highly permeable porous medium are sensitive to boundary conditions. Small temperature perturbation may change the symmetry, the cell numbers and directions, and the time required to reach steady state. This should be noted during potential field study and application of air convection.
4. Temperature fluctuations may occur near heating sources during convection under a certain level of Rayleigh numbers, and may include time-dependent oscillatory instabilities.
5. Localized heating or cooling can stabilize convective patterns even under high Rayleigh numbers, but reduces heat transfer rates because of less heat input or extraction under the same test conditions.

6. Magnitudes of convective air flow velocity are related with flow directions.
7. Critical temperature gradients are related to the effectiveness of convection. Small gradients may result in ineffective air convection.
8. The study was carried out under unique experimental conditions. Additional testing is required to study the effect of particle shape, material, density and test scale.

As an efficient and economical passive cooling approach, convective cooling is suitable for use in relatively long-term operation of engineering projects. It should continue to be investigated experimentally and numerically to become more widely spread.

ACKNOWLEDGEMENTS

The authors would like to acknowledge the research project funding from Research Fund led by Dr. David C. Sego, and the assistant from the laboratory technicians, Christine Hereygers and Steve Gamble, at the Geotechnical Centre of the University of Alberta. In addition, the first author thanks Dr. Fernando Junqueira for his valuable comments on this paper, and Golder Associates Ltd. for the encouragement and support.

REFERENCES

Arenson, L.U., Chen, J., Pham, H., and Sego, D.C. 2007. Laboratory investigations on air convection in porous media, Proceedings of *the 60th Canadian Geotechnical Conference*, Ottawa. pp. 340.

Arenson, L.U., and Sego, D.C. 2007. Protection of mine waste tailing ponds using cold air convection, In *Assessment and Remediation of Contaminated Sites in the Arctic and Cold Climates (ARCSACC)*, Edited by K. Biggar, G. Cotta, M. Nahir, A. Mullick, J. Buchko, A. Ho, and S. Guigard. Edmonton, AB, Canada. May 7-8, 2007, pp. 256-264.

Cheng, G.D., Lai, Y., Sun, Z., and Jiang, F. 2007. The "thermal semi-conductor" effect of crushed rocks, *Permafrost and Periglacial Processes*, 18 (2): 151-160.

Cheng, G.D., Sun, Z.Z., and Niu, F.J. 2008. Application of the roadbed cooling approach in Qinghai-Tibet railway engineering, *Cold Regions Science and Technology*, 53 (3): 241-258.

Goering, D.J., and Kumar, P. 1996. Winter-time convection in open-graded embankments, *Cold Regions Science and Technology*, 24 (1): 57-74.

Goering, D.J. 1998. Experimental investigation of air convection embankments for permafrost-resistant roadway design, In *Seventh International Conference on Permafrost*, Edited by A.G. Lewkowicz and M. Allard. Yellowknife, NWT, Canada. June 23-27, 1998, Collection Nordicana, 57: 319-326.

Goering, D.J. 2002. Convective cooling in open rock embankments, Proceedings*, 11th International Conference on Cold Regions Engineering, ASCE*, Reston, Va., 629–644.

Goering, D.J. 2003. Passively cooled railway embankments for use in permafrost areas, *Journal of Cold Regions Engineering*, 17 (3): 119-133.

Goering, D.J., Instanes, A., and Knudsen, S. 2000. Convective heat transfer in railway embankment ballast, In *International Symposium on Ground Freezing and Frost Action in Soils*, Louvain-la-Neuve, Belgium. pp. 31-36.

Harris, S.A., and Pedersen, D.E. 1998. Thermal regimes beneath coarse blocky materials, *Permafrost and Periglacial Processes*, 9: 107-120.

Horne, R.N., O'Sullivan, M.J. 1978. Origin of oscillatory convection in a porous medium heated from below, *Physics of Fluids*, 21, Issue 8: 1260-1264.

Jørgensen, A.S., Doré, G., Voyer, É., Chataigner, Y., and Gosselin, L. 2008. Assessment of the effectiveness of two heat removal techniques for permafrost protection, *Cold Regions Science and Technology*, 53 (2): 179–192.

Kladias, N., and Prasad, V. 1990. Flow transitions in buoyancy-induced non-darcy convection in a porous medium heated from below, *ASME Journal of Heat Transfer,* 112: 675-684.

Ma, W., Feng, G.L., Wu, Q.B., and Wu, J.J. 2008. Analyses of temperature fields under the embankment with crushed-rock structures along the Qinghai-Tibet railway, *Cold Regions Science and Technology*, 53 (3): 259-270.

Nield, D.A., and Bejan, A. 1999. *Convection in porous media*, 2nd Edition, Springer, New York.

Pham, H.N., Sego, D.C. Arenson, L.U., Blowes, D., and Smith, L. 2008. Convective heat transfer in waste rock piles under permafrost environment, Proceedings of *the 61th Canadian Geotechnical Conference*, Edmonton, AB, Sept. 21-24, pp. 947-947.

Sun, Z., Ma, W., and Li, D. 2005. In situ test on cooling effectiveness of air convection embankment with crushed rock slope protection in permafrost regions, *Journal of Cold Regions Engineering*, 19 (2): 38-51.

Wu, Q., Lu, Z., Zhang, T., Ma, W., and Liu, Y. 2008. Analysis of cooling effect of crushed rock-based embankment of the Qinghai-Xizang Railway, *Cold Regions Science and Technology*, 53 (3): 271-282.

Xu, J., and Goering, D.J. 2008. Experimental validation of passive permafrost cooling systems, *Cold Regions Science and Technology,* 53(3): 283-297.

Yu, W.B., Lai, Y.M., and Zhang, X.F. 2004. Laboratory investigation on cooling effect of coarse rock layer and fine rock layer in permafrost regions, *Cold Regions Science and Technology*, 38 (1): 31-42.